

A Two Phase Model of Oxygen Transport in Cerebral Tissue

Shen-Wei Su, Stephen J. Payne

Abstract—The dynamics of oxygen transport in the human brain are crucial to its response to local mismatches between flow and metabolism, such as occur in vascular dementia. We propose here a two phase continuum model, based on the coupled behaviour of oxygen transport in tissue and blood, which we use to simulate micro-strokes. The two phase coupled model is based on the assumption of porous media, being described by Darcy’s equation for blood flow and the mass transport equation for oxygen. Simulation results suggest that the flow input is of importance to maintain the oxygen level at the remote region from the arterial-capillary junctions.

I. INTRODUCTION

The microvascular bed is the place where nutrient and waste exchange takes place and some diseases, including vascular dementia, are believed to be caused by the mismatch of nutrient supply and uptake at this scale. Thus, many attempts have been made in theoretical and experimental studies to understand the interaction between haemodynamics and oxygen transport in biological tissues. The classical work in modelling the microcirculation was performed by Krogh [1] who suggested that the haemodynamic unit of the microvascular bed is like a bundle of tissue cylinders. Numerous other researchers have continued this work, with some studies trying to model the network behaviour in detail by considering its topology and geometry [2][3].

The blood transported in the vascular network surrounded by biological tissue, however, could be modelled by a porous flow-fluid passage only taking place in a finite permeable region in the space (see for example, Khaled and Vafai [4]). We thus treat brain tissue as a porous media by taking the vascular network as the voids or small tubes in porous media, under the low flow rate condition; we can then describe blood flow motion in the vessel-tissue system by Darcy’s Law, which relates linearly the pressure drop across the media to flow velocity. This elegant formulation has been widely used in biomedical fields [5] [6].

As for the porous features of flow transport, mass diffusion in biological tissue also bears the same similarity in the transport difference between permeable and impermeable regions in biological tissue. Nicholson [7] gave a very comprehensive

review in diffusion and relevant mechanisms in brain tissue but how the blood flow patterns affect the oxygen transport was not sufficiently addressed. To bring the linkage between haemodynamic and oxygen diffusion in brain tissue, the two phase treatment inspired by Lee and Vafai [8] is incorporated to current model to deal with the blood –tissue coupled behaviour.

II. EQUATIONS

A. FLOW EQUATIONS

Oxygen carried by the blood is transported within the network as if the flow is only allowed to move around in the void space in a porous medium. Thus, to describe the oxygen delivery system we can treat the brain tissue as a homogenous porous media and the flow is described by its locally volume averaged value. Due to the low flow velocity in the actual capillary network, the steady state blood flow motion in tissue can be taken to be governed by Darcy’s flow equations [9]:

$$\mathbf{q} = -\frac{\mathbf{K}}{\mu} \nabla P = \frac{\mathbf{V}}{\phi}, \quad (1)$$

where \mathbf{q} and ∇P are the Darcy velocity and the pressure gradient respectively. \mathbf{V} is the flow field and ϕ is the porosity. The Darcy velocity is divided by porosity to refer to the fact that only a fraction of the total volume is available for flow. Generally, in the three dimensional case, the permeability \mathbf{K} is a second order symmetric tensor, which reflects the directional diffusion transport heterogeneity due to the local variations in the microvasculature. However, we begin here by taking \mathbf{K} to be a constant under the assumption of an isotropic medium.

B. MASS TRANSPORT EQUATIONS

We consider the coupled flow-tissue system as a two phase flow system, including the blood flow perfusion through all areas occupied at a volume fraction of ϕ_b with the tissue represented by static fluid with volume fraction ϕ_t , ($\phi_b + \phi_t = 1$) as shown below:

$$\phi_b \left(\frac{\partial C_b}{\partial t} + (\mathbf{V} \cdot \nabla) C_b \right) = G, \quad (2)$$

S. W. Su and S.J. Payne are with the Department of Engineering Science, University of Oxford, Oxford, OX1 3PJ (e-mails: shen-wei.su@eng.ox.ac.uk; stephen.payne@eng.ox.ac.uk).

$$\phi_t \frac{\partial C_t}{\partial t} = \phi_t D_t \nabla^2 C_t - \phi_t M - G, \quad (3)$$

$$G = -\phi_b D_w (2/r_e) \times (C_b - C_t). \quad (4)$$

The oxygen concentrations in blood and tissue are represented by C_b and C_t respectively, and the other variables defined below. Oxygen is carried by the blood circulating throughout the tissue domain; it is thus convection-dominated, in a similar manner to the equation derived for the tissue heat transfer problem by Lee and Vafai [8].

Since oxygen diffusion is unlike the diffusion of other chemicals in biological tissue, which can only be transported easily in the area outside cells due to the cellular barrier, there is little difference in oxygen diffusion between the cells and interstitial fluid. Thus, the oxygen diffusion in intracellular and extracellular areas is considered to be lumped together with a single tissue diffusivity, D_t . The tissue part is static, which removes the need for a convection term in Eq. 3 (see [7]). The oxygen consumption term, M , is assumed here to be constant in space and time taken from [2].

The blood-tissue oxygen transport, G , is modelled by Eq. 4, which assumes that the oxygen outflux varies linearly with the concentration drop, wall permeability, D_w , where r_e is the effective vessel radii of all the vessels. The blood and tissue oxygen transport equations are thus coupled together.

III. SIMULATION SETUP

The flow and mass transport equations are all discretised using the finite volume method, which has been widely used in solving heat and mass transfer problems [10]. The matrix is solved, using FORTRAN, in a non-stationary manner where the approximate solutions and the errors are updated each iteration until the error in the final solution is minimised. The values of the model parameters used here are given in Table 1, taken from the literature.

In the simple flow simulations considered here, two flow sources and two flow sinks with strength $3.4 \times 10^{-13} \text{ m}^3/\text{s}$ are put in a $(0.5\text{mm})^3$ cube at the following positions $((0.1,0.1,0.1); (0.4,0.1,0.4); (0.1,0.1,0.1); (0.4,0.1,0.4))$ to mimic the arteriolar inlets and venous outlets in the microvascular bed with flow input and output. The boundary conditions for oxygen transport in blood and tissue share the same setting. In y and z direction are no flux while in x is set to be a constant are set as follows:

$$C(0, y, z) = C(l, y, z) = 0$$

$$\frac{\partial C(x, 0, z)}{\partial y} = \frac{\partial C(x, l, z)}{\partial y} = 0$$

$$\frac{\partial C(x, y, 0)}{\partial z} = \frac{\partial C(x, y, l)}{\partial z} = 0$$

In the blood phase, the oxygen concentration at the sources is taken as 10mM and the initial concentration for both phases is set at 0.1mM. The oxygen concentration at the sources is composed both by that dissolved in plasma and bound to haemoglobin (approximately 0.1mM and about 10mM respectively). Since the tissue contains no haemoglobin, 0.1mM is the baseline value used here for its oxygen concentration. To simulate a mini-infarct caused by blood flow shortage, a vascular blockage is mimicked by disabling a single flow source at 200s, having allowed the model to reach equilibrium prior to this. Five symmetrically arranged points are chosen in this model to monitor the temporal behaviour of tissue oxygenation in response to this reduction. The time courses are calculated by taking the spatial average over the simulation domain at each time step.

IV. RESULT AND DISCUSSION

In Fig.1, the pressure contours of the porous flow at 200s shows that the high pressure by the flow input points drives the blood towards the two sinks, as expected. After one source is removed, the high pressure zone shrinks and no longer exhibits the spatially symmetric field found previously.

From the spatially averaged oxygenation time course as shown in Fig.2, spatial averaged blood oxygenation can be seen to be about twice that of the tissue oxygenation throughout the simulation time. Both curves rise up rapidly to an equilibrium state, dropping sharply as the flow blockage occurs, finally settling down to a new steady state.

The concentration contours for blood and tissue phases are shown in Fig.3 and Fig.4 respectively. The concentration distributions for both cases share similar geometric features, and their oxygen levels decay gradually with the distance to the two sinks. Oxygen is transported further in the blood phase since its contours cover a larger area than do those in the tissue, due to convection, and a higher oxygen level can be found in the region closed to sources. After one flow source is disabled, oxygen in the surrounding area cannot be sustained, declining dramatically to the base line value (0.1mM). The significance of the flow source can be found in the mass transport in brain tissue. The convective transport is not sufficient to bring oxygen to sites remote from the supply, even at this length scale, leading to a significant oxygen shortage.

Fig.5 shows the time course of tissue oxygenation levels at the centre point C0 (0.5,0.5,0.5) and other four points C1-C4((0.1,0.175,0.4); (0.4,0.175,0.1); (0.1,0.375,0.4);

(0.4,0.375,0.1)) in the cube. Before the source removal, two pairs of curves coincide with their counterparts due to the symmetric arrangement. After one of the sources is removed, the coinciding curve pairs (C1-C2; C3-C4) diverge over time, the curve near the removal source having a larger drop than that of its symmetric counterpart. Comparison between the curves for C1 and C3 also indicates that the closer the point is to the removal source, the larger concentration drop it will have after a flow reduction.

V. CONCLUSION

The two phase porous media model is presented here to simulate the flow and oxygen transport in brain tissue. The time history for averaged oxygenation for both blood and tissue reveals synchronized system states while that for tissue oxygenation at different locations share the similar state transition patterns. As the flow blockage occurs, the region near removal source is unable to maintain sufficient oxygen supply, leading to great decrease in oxygen level. This indicates the strong influence of the *local* microvascular blood supply on the oxygen transport in tissue, which means the detail of microvasculature is of importance due to its impact on blood supply. Hence, detailed study for vascular properties is a valuable input in future simulation and has been conducted by Su et al.[11].

At this stage, due to the lack of information concerning the flow rate and locations of the artery-capillary and venule-capillary junctions, we cannot interpret the exact nature of this flow yet. In addition, the permeability, porosity and oxygen diffusivity in tissue need to be considered in more detail in the light of physiological measurements to bring a more detailed and accurate understanding of the real system.

REFERENCES

- [1] A. Kough, 1921, Studies on the physiology of capillaries. II. The reactions to local stimuli of the blood vessels in the skin and web of the frog. *J. Physiol.* 55:414–422.
- [2] D. A. Beard and J. B. Bassingthwaite, 2001, Modeling advection and diffusion of oxygen in complex vascular networks, *Ann. Biomed. Eng.* 29 : 298–310.
- [3] T. W. Secomb, R. Hsu, E.Y.H. Park, and M. W. Dewhirst, 2004, Green's function methods for analysis of oxygen delivery to tissue by microvascular networks. *Ann. Biomed. Eng.* 32: 1519-1529.
- [4] Khaled, A.-R.A., Vafai, K., 2003, The role of porous media in modeling flow and heat transfer in biological tissues *Int. J. Heat Mass Transfer* , 46 (26), 4989-5003.
- [5] W.J. Vankan, J.M. Huyghe, J.D. Janssen, A. Huson, W.J.G. Hacking, W. Schreiner, 1997, Finite element analysis of blood flow through biological tissue, *Int. J. Eng. Sci.* 3 [1] 375–385.
- [6] J.M. Huyghe, D.H. Vancampen, 1995, Finite deformation-theory of hierarchically arranged porous solids. 2. Constitutive behavior, *Int. J. Eng. Sci.* 33 1873–1886.
- [7] C. Nicholson, 2001, Diffusion and related transport mechanisms in brain tissue, *Rep. Prog. Phys.* 64, 815–884.
- [8] D.Y. Lee, K. Vafai, 1999, Analytical characterization and conceptual assessment of solid and fluid temperature differentials in porous media, *Int. J. Heat Mass Transfer* 42, 423–435.
- [9] H.R.P.G. Darcy, 1856, Les Fontaines Publiques de la ville de Dijon, Vector Dalmont, Paris.

- [10] S. V. Patankar, 1980, Numerical Heat Transfer and Fluid Flow, Hemisphere, Washington, DC. USA.
- [11] S. Su, M. Catherall and S. Payne, 2009, A novel computational algorithm for the generation of network models based on statistical properties, Manuscript in preparation.

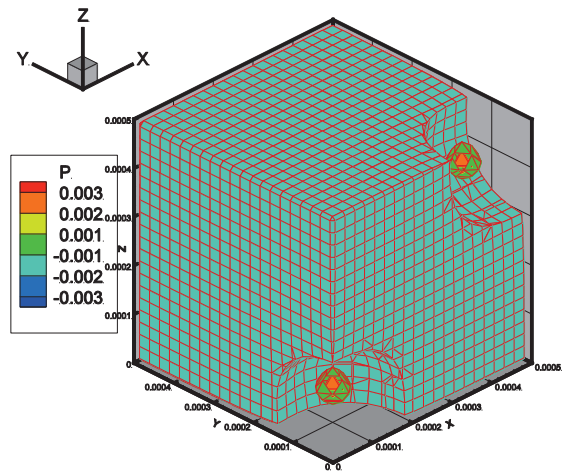


Fig. 1 Pressure field in the porous media flow: above is the contour at 200s; below the contour at 400s

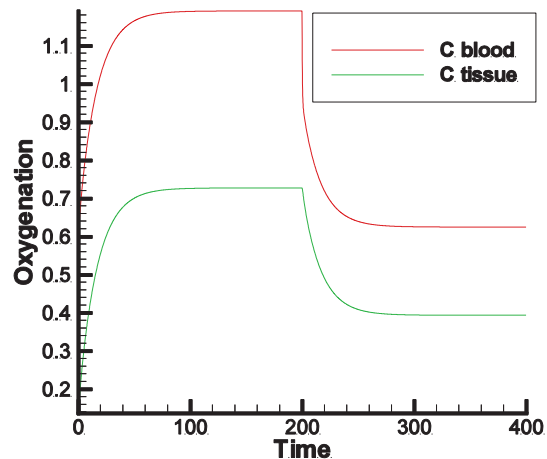
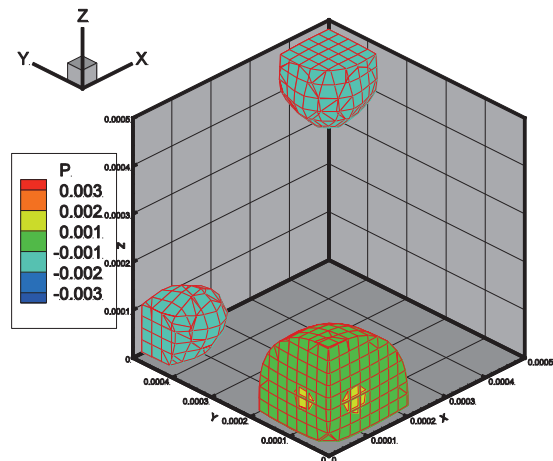


Fig. 2 . Time course of spatially averaged blood and tissue oxygenation

TABLE I
UNITS FOR PROPERTIES

Symbol	Quantity	Unit
μ	Blood dynamic viscosity	3×10^{-3} kg s/m
D_w	Wall oxygen permeability	5.5×10^{-6} m/s
D_t	Tissue oxygen diffusivity	1×10^{-9} m ² /s
K	Permeability	1×10^{-9} m ²
M	Oxygen consumption	0.005 mM/s
φ	Porosity	0.03
Φ_b	Blood volume fraction	0.03

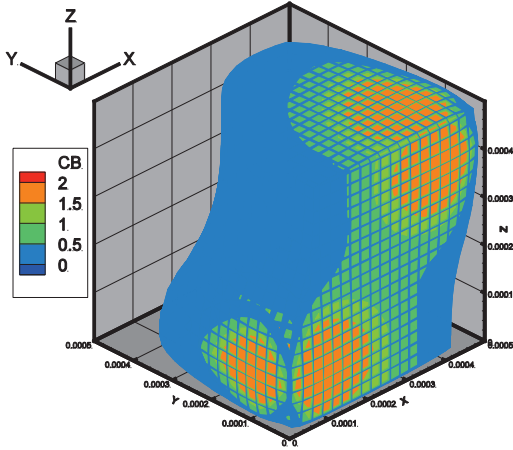


Fig. 3 . Oxygen contour of the blood phase: above is the contour at 200s; below the contour at 400s

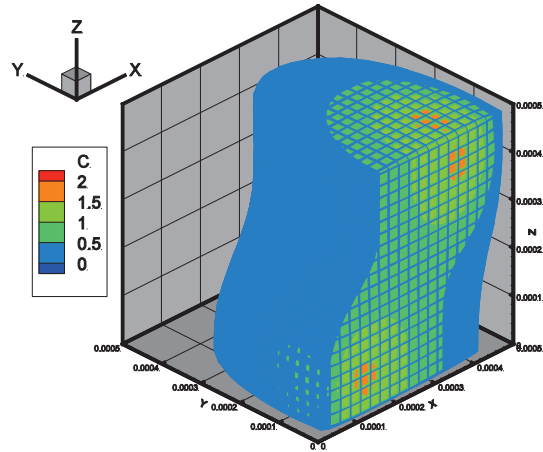
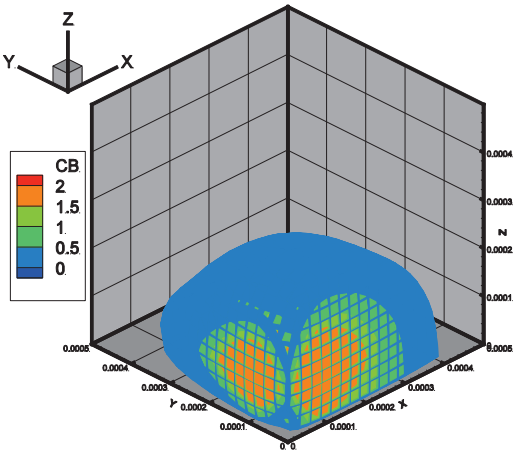


Fig. 4 . Oxygen contour of the tissue phase: above is the contour at 200s; below the contour at 400s

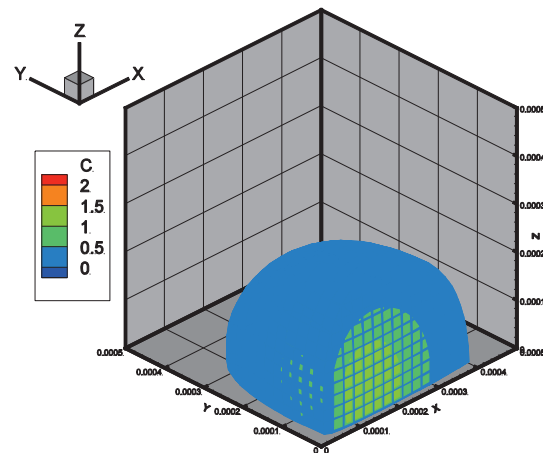
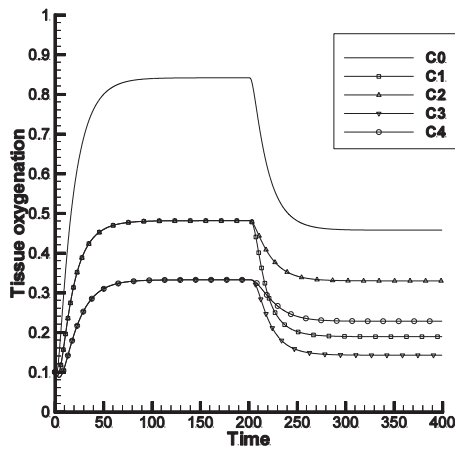


Fig. 5 . Time course of oxygenation at different points in the tissue